

ROCK MASS CHARACTERIZATION FROM SEISMIC MEASUREMENTS

by Nick Barton
Visiting Professor, USP, São Paulo, Brazil
Technical Adviser, NGI, Oslo, Norway

1. INTRODUCTION

“Nature has left us an incomplete and often well-concealed record of her activities, and no “as constructed” drawings”! These introductory remarks from Stapledon and Rissler (1983) who were General Reporters at the ISRM Congress in Melbourne can be utilized as one of the justifications for performing geophysical surveys. Before drilling begins at a site we must produce preliminary plans of investigation that will produce useful guidelines for the next more detailed stage of investigation. If a model is already available for converting seismic velocities into preliminary rock engineering data (rock quality, deformability, rock support needs, etc.) we can focus the next phase of drilling and associated testing more clearly on a set of objectives. The objectives will generally be to optimise the safety and economy of that which is to be constructed. Low velocity and potentially high permeability zones will be the natural focus of attention, though in a TBM tunnelling project we may also be concerned by too much high velocity rock, due to the slow progress made in hard, sparsely jointed rock.

In this connection, a velocity of 2.5 km/sec for massive chalk marl of high porosity will have entirely different consequences to that of a regional fault of the same velocity crossing a Japanese high speed rail tunnel, and delaying progress by months, while world record speeds of boring are achieved in the chalk marl, perhaps even 1.5 km/month. The natural velocity of the unjointed rock under in situ conditions (Sjøgren et al. 1979), and the contrast seen in low velocity zones is the main index of difficulty, since an order of magnitude reduction in Q-value (rock quality) may accompany each 1.0 km/sec reduction in seismic velocity.

2. SHALLOW REFRACTION SEISMIC

Shallow refraction seismic measurements for measuring first arrival, compressional P-wave velocities close to the surface can give a remarkable picture of near surface conditions due to some fortuitous interactions of physical phenomena. Firstly, weathering and the usual lack of significant stress near the surface has allowed joint systems, shear zones and faults to be exaggerated in both their extent and severity. Secondly stress levels are low enough to allow joints and discontinuities to be seismically visible due to their measurable apertures. So-called acoustic closure occurs at greater depths than those usually penetrated by conventional hammer seismic, unless rock strengths are rather low.

The example of joints in chalk marl at the Chinnor Tunnel in the UK closing at about 15 meters depth (Hudson et al. 1980) to give a stable 1.6 km/sec field velocity (Figure 1) can be contrasted to the saturated joints in gneiss at the Gjøvik cavern in Norway, which gave a continuous rise in velocity from 3.5 to 5.5 km/sec in the first 50 meters depth due to increased stress, yet had almost unchanged rock quality (Barton et al. 1994).

The latter is an example of the need to interpret seismic velocity with knowledge of depth and/or stress level, since a Q-value increase from perhaps 1 to 100 might otherwise be assumed in these first 50 meters.

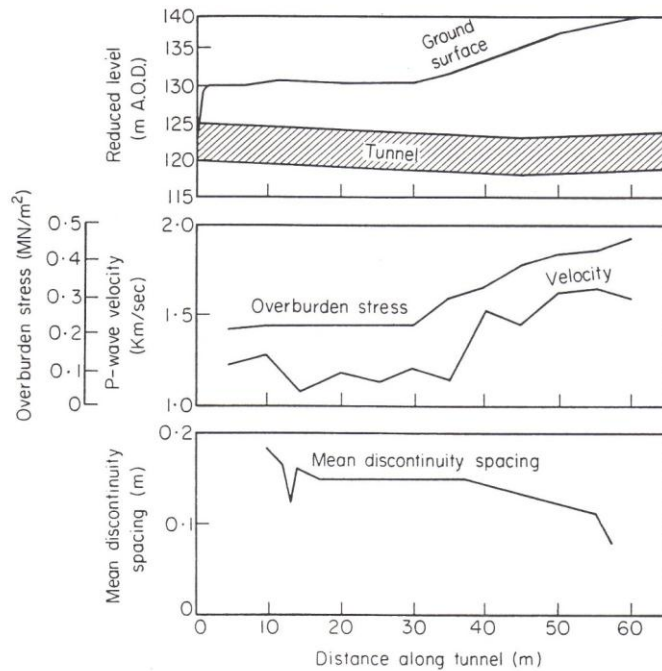


Figure 1. Velocity increase at the Chinnor Tunnel in Chalk, due to increase of overburden, despite greater joint frequency. Hudson et al., (1980).

The Chinnor Tunnel example really emphasised the influence of stress level on “acoustic closure”. In the first 10-15 meters increase of overburden above the tunnel the velocity rose from 1.2 to 1.6 km/sec despite an increase in joint frequency. The expected reduction in velocity was masked by the greater influence of stress-induced joint closure. A third factor in the general success of shallow refraction seismic (or of shallow cross-hole seismic tomography) is the greater “visibility” of unsaturated or dry joints in the rock mass, should the ground water level be low.

3. PRELIMINARY CORRELATIONS OF VELOCITY AND QUALITY

Due to the seismic “visibility” of jointing in the upper 25 to 30 meters, Sjøgren et al. (1979) and Sjøgren (1984) were able to record significant correlations between V_p , RQD and joint frequency. Since their measurements were shallow, the effect of stress-induced joint closure was minimized. They also effectively removed other sets of variables by generally recording correlations for hard and almost unweathered igneous and metamorphic rocks. The variables of depth, porosity, uniaxial compressive strength and density were therefore largely removed. The V_p , RQD and Fm^{-1} (joint frequency per meter) data in Figure 2 is that derived by Sjøgren et al. (1979), who analysed 120 km of seismic traces and compared measured velocities with jointing (RQD and joint frequency F , m^{-1}) in 2.8 kilometers of drill core recovered from the same hard-rock locations. Quite consistent trends between low V_p values and low RQD (%) and high F (m^{-1}) were obtained. When velocities were high (such as 6 km/sec) RQD generally was approaching 100% and there were few joints per meter of core. The rock types involved in the Sjøgren et al. 1979 studies were granite, gneiss, amphibolite, pegmatite, meta-amorphosite, porphyry, quartzite and mylonite.

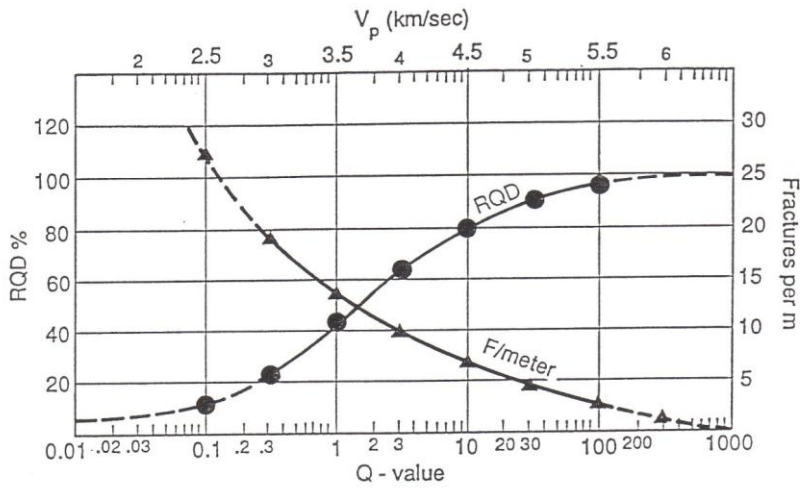
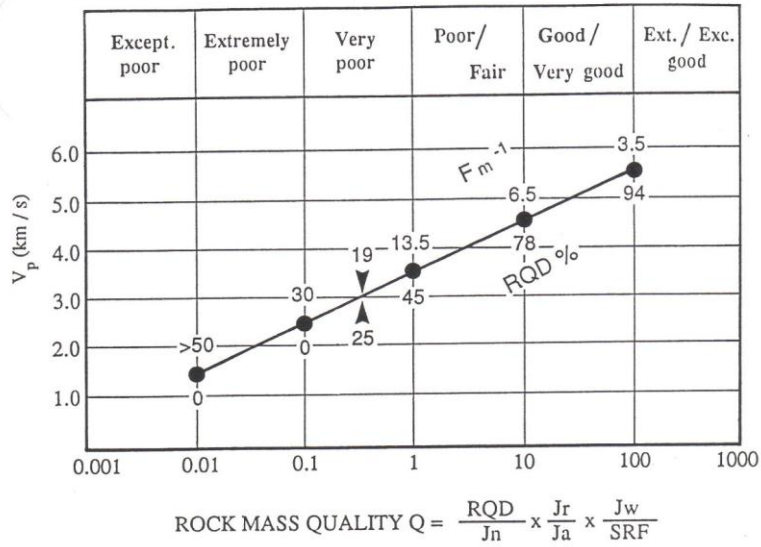


Figure 2 (a), (b). RQD and $F m^{-1}$ (joints per meter) from Sjøgren et al. (1979). V_p - Q relation for hard, near-surface, unweathered rocks from Barton et al. (1992).

On the basis of NGI's cross-hole seismic tomography measurements at the Gjøvik (62 m span) cavern site in Norway, and Q-logging of the same boreholes, a preliminary model for a V_p - Q relationship was developed (Barton, 1991). This was subsequently confirmed by analysis of several other seismic, cross-hole and Q-logs including the Xiaolangdi (Yellow River) hydro electric project, where plate loading tests also provided deformation modulus measurements that showed broad correlation with Q-values logged by the writer. Various hard rocks such as granites, gneisses, tuff and competent sandstones were also tested in projects in Norway, England and Hong-Kong, where first-hand information on Q-logging was available.

The proposed relationship between V_p (km/sec) and Q-values shown in Figure 2, is for hard rock

sites, and has the simple form: $V_p = 3.5 + \log_{10} Q$. When the Q-value is 1.0, mid-range between 0.001 and 1000, $V_p = 3.5$ km/sec, and it changes by roughly 1 km/sec (upwards or downwards) for each ten-fold change in Q-value. (Barton et al. 1992). This model has now been tested on sites in several countries where Q-logging of core has been performed. The fit to measured data is quite good, provided that depths are shallow (i.e. down to 25 m, near the limit of refraction seismic surveys) and provided that the rocks are non-porous and reasonably hard (i.e. uniaxial strengths of 100 MPa or more). This model for hard rocks, and a modified one for soft porous rocks to be developed later, can be used for initial interpretation of seismic data.

The most typical use of seismic velocity information at a site is in the prediction of depth to bedrock and of low velocity zones. The collection of shallow refraction seismic measurements in Figure 3 from Sjøgren 1984, emphasises the richness of potential information, especially if velocities can be converted to a rock quality estimate, using relationships such as the above Q - V_p coupling for hard, unweathered rocks.

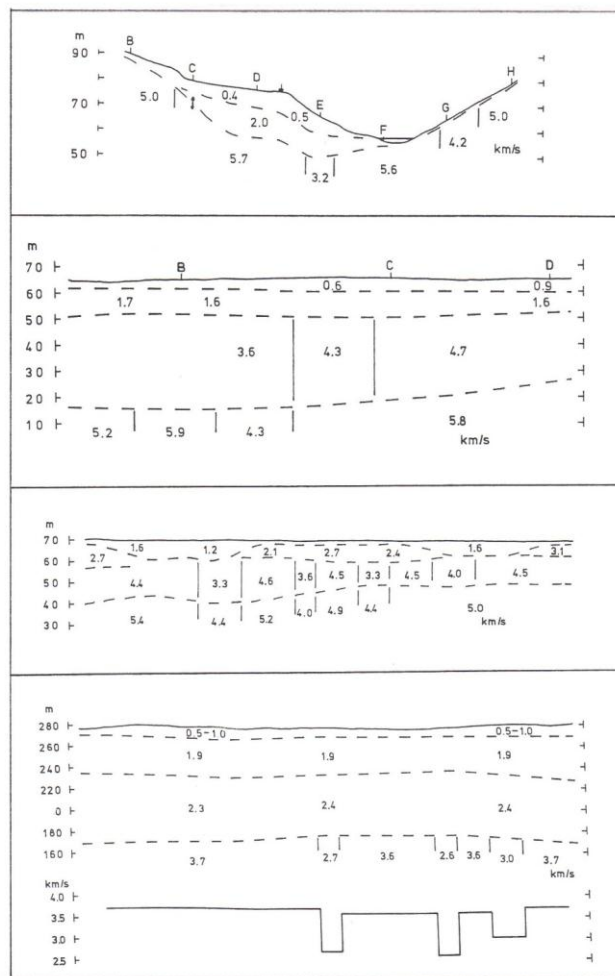


Figure 3. Some examples of shallow refraction seismic. Interpretations at sites with low velocity zones. Sjøgren, (1984).

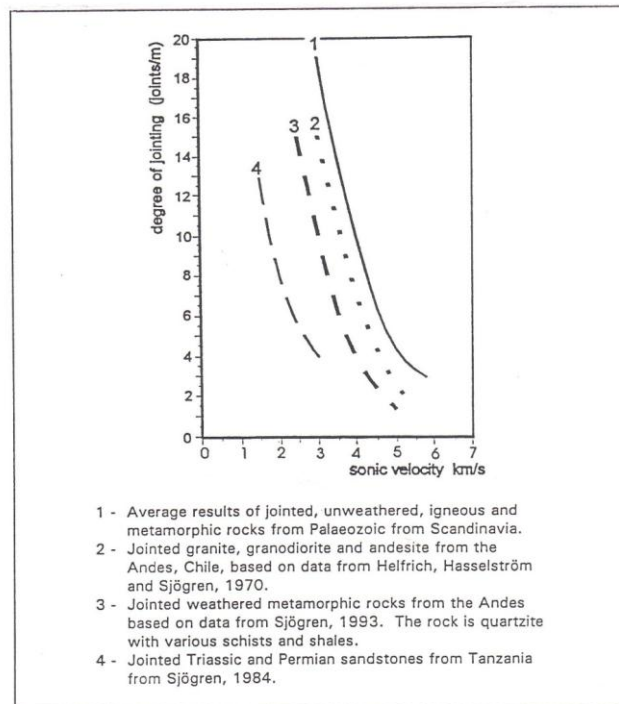


Figure 4. Seismic data from Sjøgren et al. (1979) and Helfrich et al. (1970). Figure completed by Palmstrøm (1996), from unpublished Sjøgren data.

4. POTENTIAL PITFALLS IN VELOCITY AND QUALITY CORRELATIONS

There are several reasons why joint frequency ($F \text{ m}^{-1}$) and velocity (V_p) correlations need to be carefully scrutinized. Firstly, when there is a tendency for weathering, or for matrix porosities higher than normal for hard rocks, then the same joint frequency will be recorded at lower seismic velocities. The four curves in Figure 4 represent, at the one extreme (curve No. 1) the same data as given in Figure 2 for hard, unweathered rocks at shallow depth. The degree of weathering increases, rock strength reduces, and the matrix porosity increases while progressing from curve No. 1 to 2 to 3 to 4 in Figure 4. The data has been assembled from Sjøgren and co-workers data by Palmstrøm 1996, and is derived from measurements in Scandinavia, in the Andes and in Tanzania. Corrections for weathering, porosity and rock strength (or density) are needed to explain the range of data.

Velocity-joint frequency data can also correlate to the right-hand side of curve No. 1 (Figure 4), if overburden or stress effects cause partial “acoustic closure” of the joints. In such cases, a higher P-wave velocity will be recorded despite the large joint frequency recorded in drill core.

The extensive data of Niini and Manuen, 1970 which is shown in Figure 5, was derived from 55 vertical or steeply inclined holes drilled into the upper 15 meters of bedrock, along 100 km of seismic traces for the 120 km long Helsinki water supply tunnel. The complication of increased stress, from tectonic causes or from 15 to 30 m of additional soil cover, meant that high joint frequencies were recorded even when velocities were as high as 4.5 km/sec.

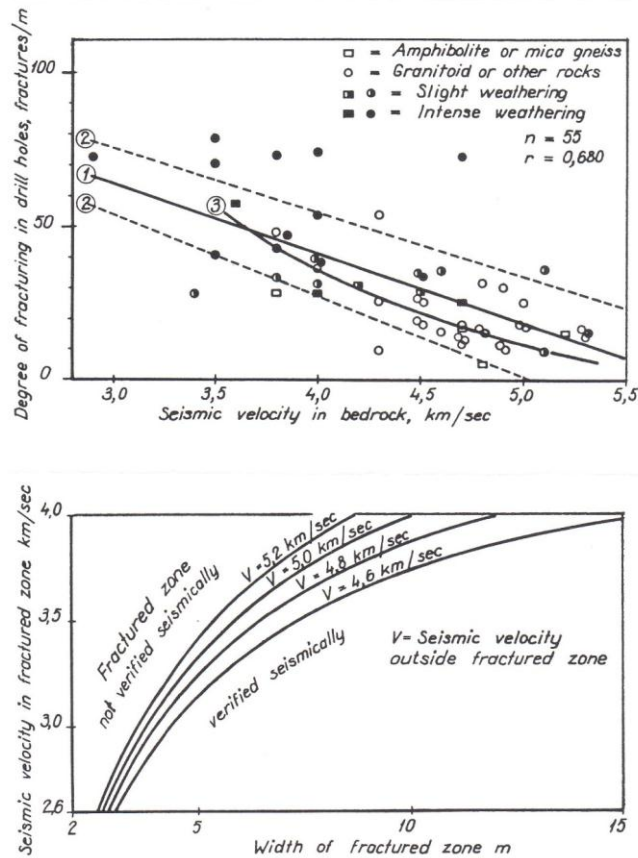


Figure 5. Correlation of joint frequency, fracture zone widths and V_p from 55 boreholes and up to 100 km of seismic traces from the Helsinki region, Finland. Niini and Manunen, (1970).

New and West (1980) performed investigations both in the laboratory and in a tunnel driven in sandstones and mudstones, in order to investigate “acoustic closure” more closely. Their laboratory tests of 0 to 3 MPa loading of artificial flat rock surfaces under dry conditions, suggested “acoustic closure” (or more or less constant velocities) at about 2 to 3 MPa, and perhaps lower values of stress for softer rocks. Hudson et al. (1980) tests on joints in weak chalk marl were consistent with this picture, and indicated that stresses as low as even 0.4 MPa were sufficient. Tanimoto and Ikeda (1983) found that V_p was proportional to the normal stress applied to simulated joints over the range 3 to 20 MPa, but that V_p dropped rapidly below stress levels of 3 MPa. A cut-off aperture of about 40 μm separated their experimental results, with apparently no influence of $F \text{ m}^{-1}$ on V_p below this aperture. The above effects and new experimental data are the main reason why Tanimoto and Kishida (1994) and others are advocating the use of compression wave amplitude as a supplement to velocity data, for better sensitivity to jointing at higher stress levels than those usually employed in shallow refraction seismic.

5. THE INFLUENCE OF MATRIX POROSITY AND STRENGTH ON SEISMIC VELOCITY

There is a wealth of data in the literature concerning the effect of the rock matrix porosity on the P-wave velocity. In general, proportionality is found. A classic set of experimental data is that provided by Fourmaintraux (1975), which is reproduced in Figure 6. The strong influence of the porosity of the matrix in rocks such as limestone and sandstone and the linear nature of the V_p - $n\%$ relationship is clearly demonstrated. In the case of the granites, where joint porosity and presumably, weathering of the matrix are the chief sources of porosity, the reduction of velocity is even more marked. The uniaxial compressive strength is also strongly related to matrix porosity in the case of porous rocks such as limestones and sandstones. It may therefore be logical to allow for the influence of both σ_c and $n\%$ when designing an integrated V_p - rock quality - deformability chart.

The laboratory data for weak rocks such as Tertiary mudstones and sandstones given in Figure 7, clearly requires that uniaxial strength is incorporated in any generalized integration of velocity and quality.

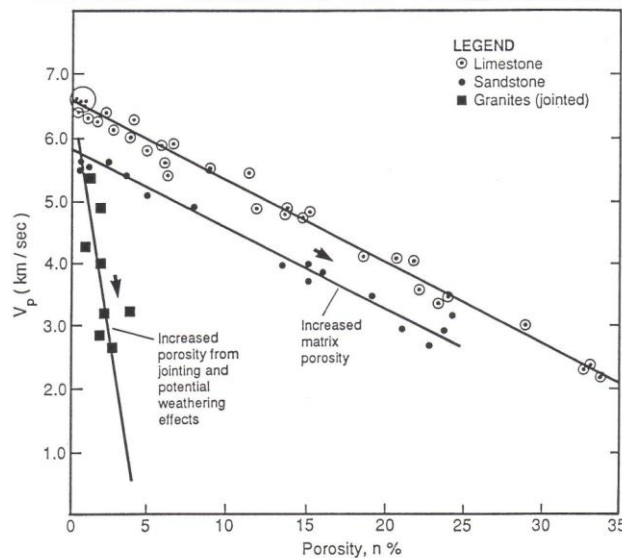


Figure 6. Linear V_p - porosity trends for limestones, sandstones and weathered granite. Fourmaintraux, (1975).

6. THE INFLUENCE OF WEATHERING AND MOISTURE ON SEISMIC VELOCITY

Effects of weathering on the seismic properties of four rock types from a dam site (quartz diorite) and from three quarries (andesite, basalt and dacite) in Japan are reported by Saito (1981). This very comprehensive study involving hundreds of samples with different weathering grades and porosities, gives a very useful picture of some key trends between strength, hardness, porosity, degree of water saturation and P-wave velocity. These behavioural trends are fundamental to an understanding of the in situ behaviour, where the addition of joints to the cracks and pores tested here, adds another layer of complexity.

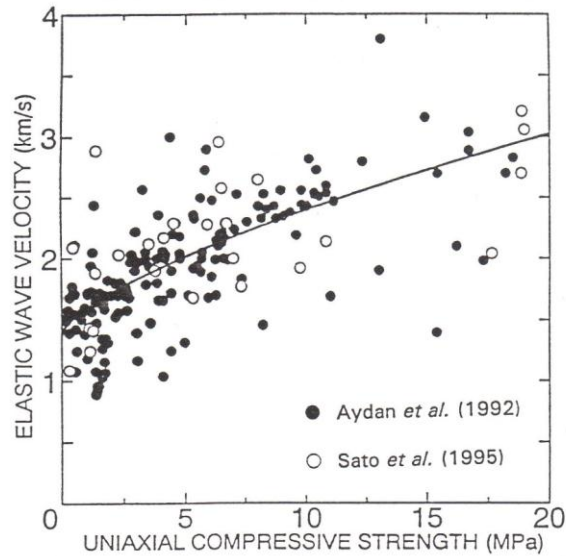


Figure 7. Laboratory relationships between V_p and σ_c for weak rocks, after Aydan et al. (1992) and Sato et al. (1995).

Saito (1981) collected numerous block samples of the different rocks and weathering grades and cast these in regular shaped concrete blocks, before taking cylindrical samples for his tests. Schmidt (N-hammer) tests were made on these larger blocks. Figure 8(a) illustrates and describes the typical weathered zones (1 to 5), and an idea of the range of compression strengths (dry samples) and porosities are given in Figure 8(b). The very different porosities of the three volcanic rocks compared to the crystalline quartz diorite are well reflected in the clear separation of the V_p values shown in Figure 8(c). The extended V_p range of < 1 km/sec to almost 6 km/sec is the result of the huge range of porosities (57% to 1%). When only uniaxial strength and velocity are plotted (Figure 8(d)) the fundamental differences in porosity are not seen due to the relatively high strength of the three volcanic rock types.

Figure 8(e) shows how the Schmidt (N) hammer relates to V_p in a quite linear manner, not showing the same "plateau" effect seen with V_p versus σ_c . The significant differences of behaviour caused by porosity reappear when degree of water saturation and its effect on V_p are shown side-by-side in Figure 9(a) and 9(b). The higher porosities corresponding to higher weathering grades show strong increases in V_p from initial low values, as saturation exceeds about 85%. Much less sensitivity to saturation (just a weak linear effect) are seen for the fresher, low porosity, high V_p samples.

7. EFFECT OF ANISOTROPY IN THE ROCK MATRIX OR IN THE JOINTING

There are several potential causes of velocity anisotropy, including stress effects on microcracks, foliation, bedding, and anisotropic joint sets. Velocity anisotropy may be caused by the effects of stress on pre-existing micro cracks, in which velocities become much higher in the direction of loading, due to microcrack closure perpendicular to the loaded direction. Velocities at right angles to the loaded direction increase at a lower rate. (Nur, 1971). Until the stresses are applied,

Zone of weathering	Friability	Features of fissure	weathering profile	
			Quartz diorite	Volcanic rocks
5	very friable with hand	Rock structure is barely retained.		
4	very friable with hammer	Cracks are filled up with debris and clay.		
3	friable with hammer	marked irregular cracks		
2	hardly friable with hammer	irregular cracks		
1	not friable with hammer	joint only		

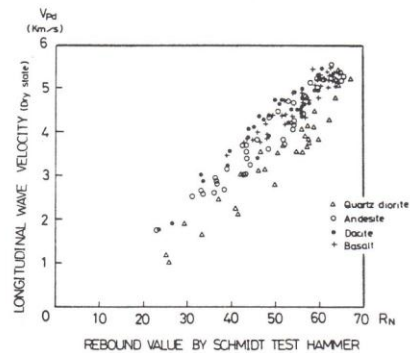
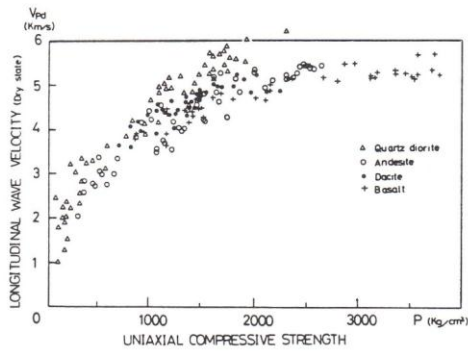
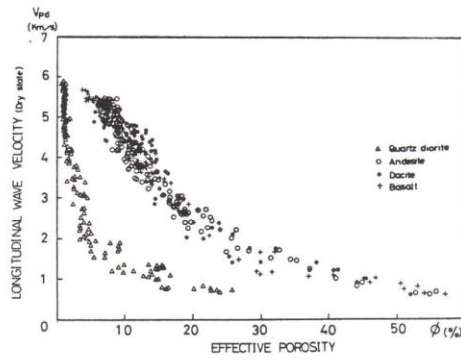
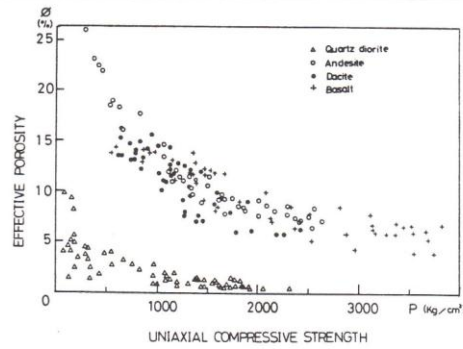


Figure 8. Effects of weathering at four sites in Japan cause huge ranges of porosity, strength and P-wave velocity. Saito, (1981).

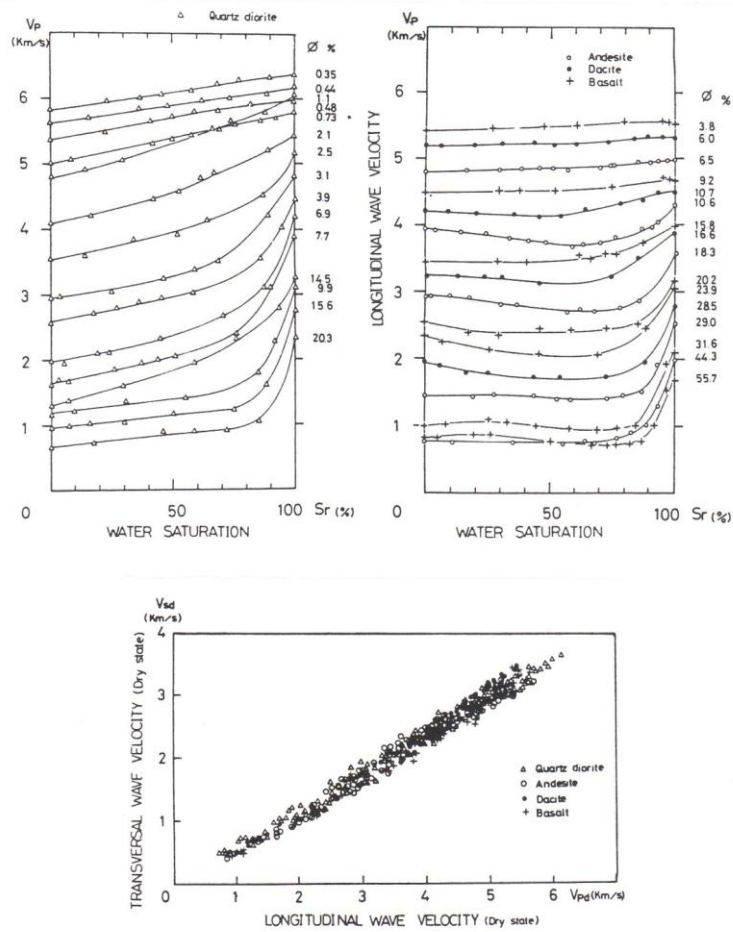


Figure 9. Top: effect of water saturation on V_p for the same four rock types. Bottom: V_s/V_p trend for all the samples, dry state. Saito, (1981).

isotropic velocity may have existed in the sample. When however a pre-existing foliation or schistosity is present, such as for the Nagra gneiss from Switzerland illustrated in Figure 10, strong velocity anisotropy may be seen, particularly when in the dry state (Hesler et al. 1996). The velocity parallel to the schistosity is almost 1.5 km/sec higher than perpendicular to the schistosity. Anisotropy reduces with stress increase in this case, compared to an increasing anisotropy with stress in the case of the microcrack closure effects noted above.

When actual flaws, cracks or joints are present, the velocity anisotropy will be strongly related to the anisotropy of orientation of the flaws, cracks or joints. These discontinuities will also reduce the velocities in general, giving both a velocity anisotropy (max. V_p parallel to dominant joints) and a reduced value of the velocity ratio V_p/V_o (where V_o is for the intact rock). Oda et al. (1986) data shown in Figure 11 is a very good example of anisotropy at laboratory and in situ scale, with marked reductions of V_p/V_o (and squared velocity ratio) in the case of the most jointed granite.

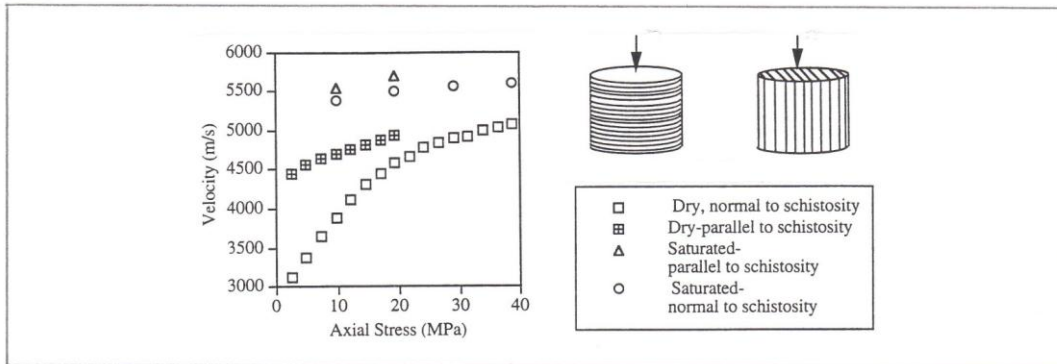


Figure 10. Effect of schistosity orientation, and dry or saturated condition, on V_p values for Nagra gneiss, Switzerland. Hesler et al. (1996).

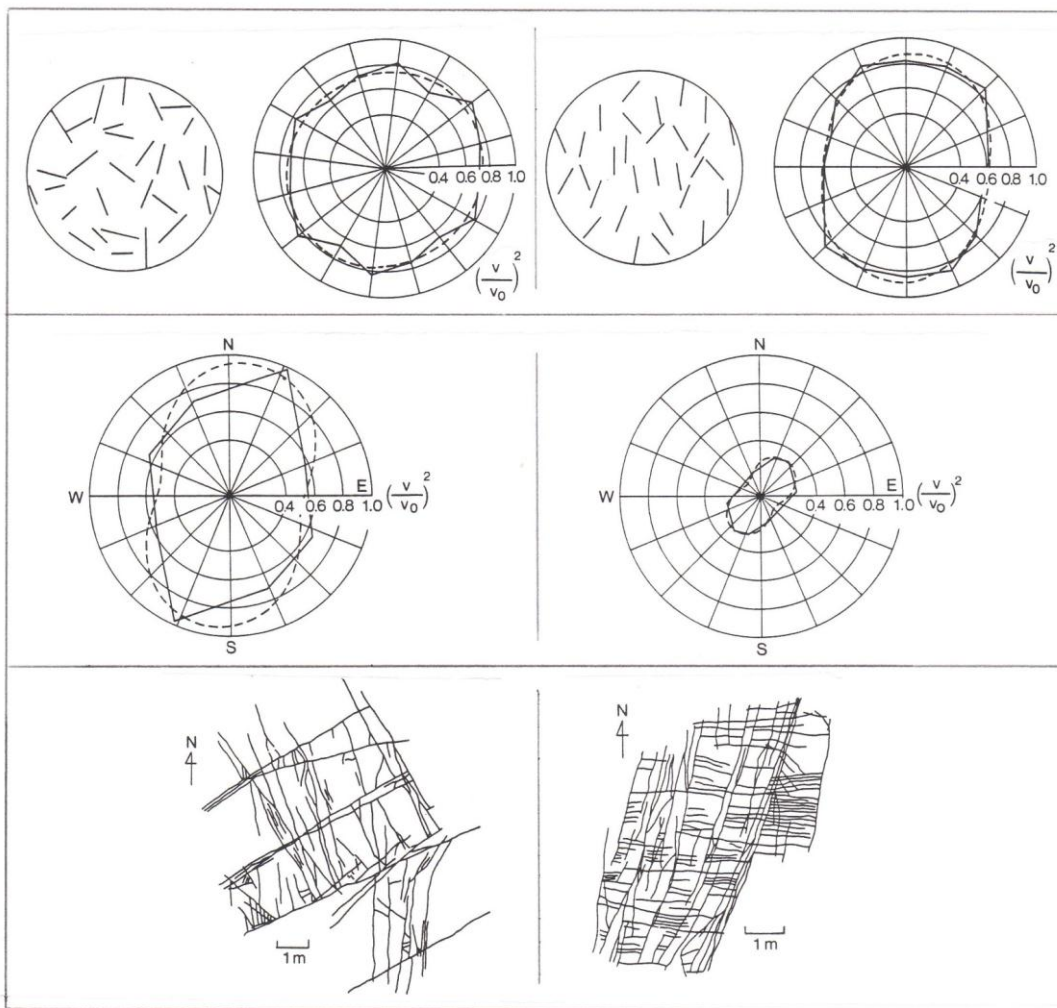


Figure 11. Velocity anisotropy of gypsum samples with flaws, and of jointed granite sites in Japan. ($V_0 = 4.5$ km/sec). Oda et al. (1986).

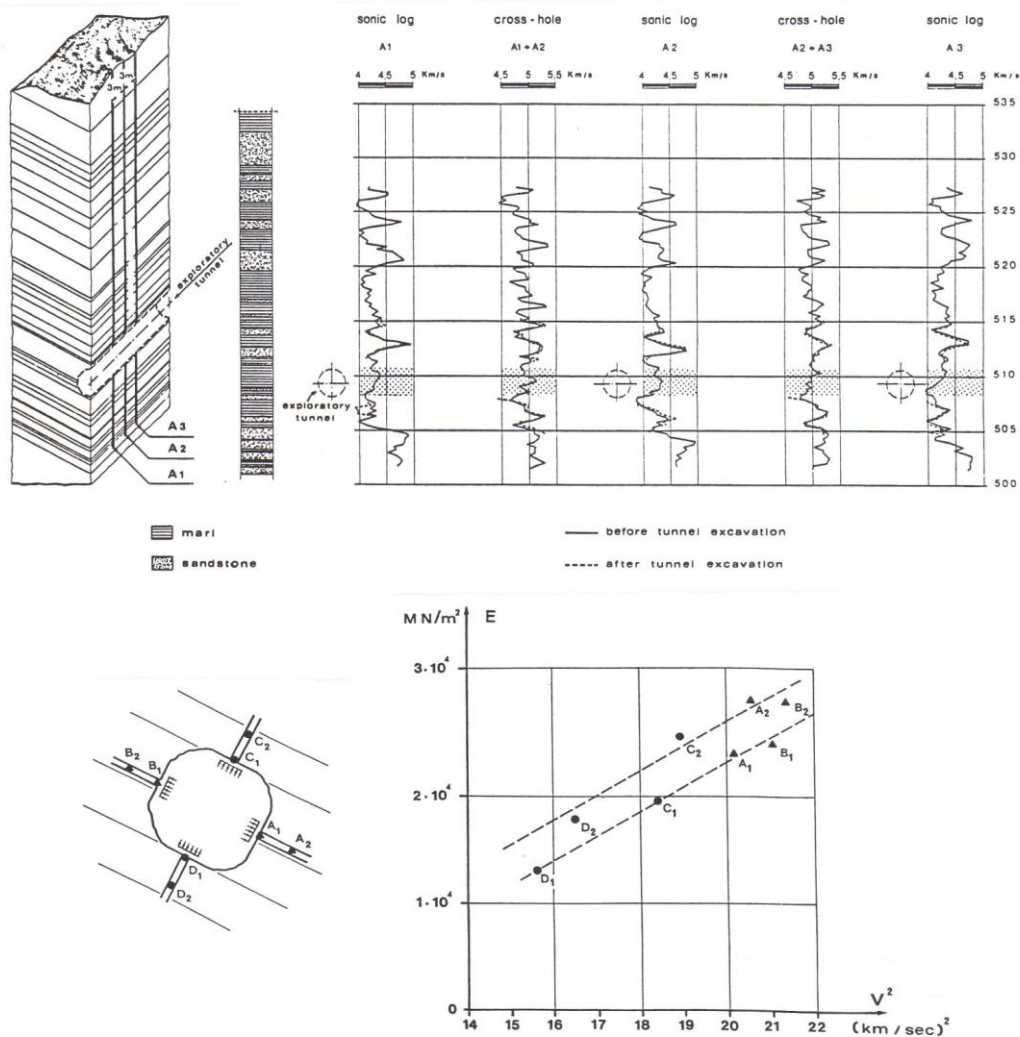


Figure 12. Anisotropy caused by inter-bedded strata of different stiffnesses (sandstones and marl). EDZ effects on moduli at different depths are also evident. Oberti et al. (1979).

In jointed chalks in England, Nunn et al. (1983) measured P-wave velocities as low as 1.8 km/sec perpendicular to dominant jointing caused by a major monocline, while parallel to the $15^\circ \pm 7^\circ$ joint direction, the velocity was at a maximum of 2.8 km/sec, in the consistent direction of 10° to 20° .

Concerning anisotropic, inter-bedded or layered rock masses and their seismic characteristics, Oberti et al. (1979) reported a very instructive set of in situ measurements that involved down-hole sonic logging, cross-hole logging and comparison with deformation moduli determined at different depths below plate loading tests. The latter were performed parallel and perpendicular to the strata, and could therefore be compared with the anisotropic velocities. The rhythmically layered sandstone and marl, with a dip of 27° , was the foundation for an arch-gravity dam in the

Apennines in Italy. Figure 12 a illustrates the geological sequence and location of boreholes. The exploratory tunnel used for the plate loading tests (Figure 12(b)) was at 3 to 35 m depth, and ran parallel to the strike of the inter-bedded strata.

The three boreholes (A1 to A3) were parallel and spaced at 3 m centres. Down-hole and cross-hole logs are shown sequentially in Figure 12(a). The mean velocity anisotropy in this orthotropic rock mass were 4.3 km/sec (perpendicular to layers) and 5.0 km/sec (parallel to the layers). Differences can be noted between the higher velocities in the sandstones and the lower velocities in the marl. Figure 12(b) shows a comparison of the sonic measurements performed in central boreholes beneath each plate loading location, where deformations were also recorded with extensometers, so that deformation moduli at different depths could be calculated. The lower moduli and lower velocities of the disturbed near-surface rock are evident, especially that of the marl in the invert, where moisture content perhaps had increased. As can be checked later, the deformation moduli and velocities measured in these tests correlate closely with the $V_p - Q - M$ model developed later, where Q-value or velocity is seen to correlate with deformation modulus, provided suitable corrections are made for porosity, rock strengths, and depth.

8. EFFECT OF ROCK STRESS AND DEFORMATION ON VELOCITY (THE EDZ)

When considering the performance of engineering structures in rock that is jointed, the effect of too low or too high stress must be expected to have effects on velocity, due to loss of confinement or excessive deformation, as the case may be. In the case of massive unjointed rock, deep tunnel excavations may cause rock failure and inevitable velocity reductions. In each of the above cases, velocity monitoring using refraction seismic or down-hole measurements (or cross-hole tomography) will enable the depth of these adverse effects, and their severity, to be estimated. In the following, examples of low stress and high stress effects will be given.

Geophysical studies of rock masses in the USSR is the subject of an interesting review by Savich et al (1983). An unusual and instructive geophysical monitoring of the Dnieper ship lock excavation, which reached a depth of more than 20 meters, is shown in Figure 13. The effect of

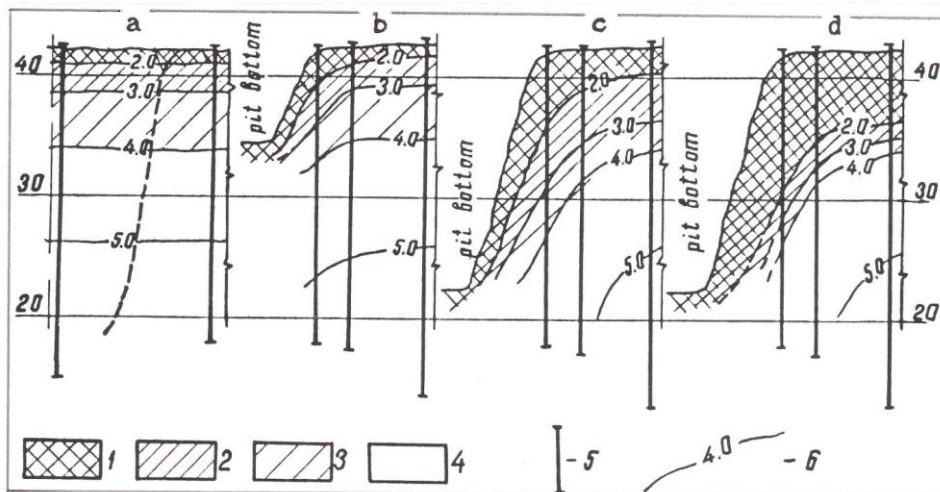


Figure 13. Effect of ship lock (slope) excavation and degradation with time on the V_p distribution. Savich et al. (1983).

loosening caused by blasting, stress relief (and presumably inadequate slope reinforcement) is shown very clearly. There is a one year delay between diagrams (c) and (d). Savich et al (1983) refer to a 200 - 300% reduction in velocity, a 75 to 85% reduction in deformation modulus, and a 1 to 20 times increase in "joint voids". This could be described as an excavation disturbed zone (EDZ) study related to slopes, in which velocity changes were related both to loosening and presumably to water draw-down. The same mechanisms may be at work around tunnels, in which EDZ effects are important for many reasons, including support needs, reduced deformation modulus, and increased leakage (or permeability). The latter two effects may be remediated for the special cases of pressure tunnels or nuclear waste repositories by pre-or careful post-grouting.

A classic EDZ investigation in relation to pressure tunnel design was reported by Kujundzic et al. 1970. They performed a trial chamber test for investigating post-stressing effects on the concrete liner of their 5 m diameter, circular tunnel. In the course of this study they utilized numerous grouting boreholes (32 in all) for conducting cross-hole seismic along the tunnel axis, at eight different radial positions. Their results are shown in Figure 14, from which they visualized the existence of three zones around the tunnel: 1. the loosened zone (with lowest velocities); 2. the stress bearing ring (with highest tangential stresses and velocities); 3. the uninfluenced zone (with declining velocities and back-ground stresses). Their mean results ($V_p = 3.5$ km/sec at the tunnel wall, $V_p = 5.5$ km/sec at 1 m radius, and $V_p \approx 4.5$ km/sec in the undisturbed zone) shown in the centre of Figure 14 must be interpreted by means of a V_p - stress effect model, to be discussed later.

In recent years, reports of EDZ investigations have become numerous in the rock mechanics literature, particularly in connection with nuclear waste repository investigations. An early model for such investigations at a dam site in Sweden was provided by Hasselstrøm et al. 1964, who compared cross-hole and down-hole sonic logging results in an investigation gallery. Velocities were seen to fall from about 5.5 to 3.5 km/sec in the outer 1 meter of their 1.5 x 2.0 m gallery. The authors cited the same reasons for the velocity reduction that we hear today at nuclear waste investigation sites such as Hanford (King et al. 1984), URL (Maxwell and Young, 1996), Aspo (Emsley et al. 1996) and Stripa. Fracture formation, joint disturbance, stress redistribution and possible dessication of the existing joint system were all listed by Hasselstrøm et al. in 1964, and are equally relevant (and complicated) today, almost 35 years later.

In relation to seismic velocity changes caused by high stress rock failure, acoustic emission (AE) or even rock bursts, the remote tomographic imaging technique represents some distinct advantages in the hostile environment of deep mines or highly stressed tunnels. Maxwell and Young (1996) have given nice examples of the combination of velocity images and AE locations, both for an experimental tunnel (URL) in ideal intact rock conditions, and in the more complex case of a medium deep (1800 m) gold mine in South Africa. At URL in Canada, known stress changes and known stress induced fracturing were matched with velocity tomograms and acoustic emission events as shown in Figure 15. The relevant elastic stress distribution calculated with a boundary element program is also shown. The location of the microseismic sensors in relation to the drilled-and-hand-mined test tunnel at URL is also shown in the figure.

The AE events were seen to cluster both where tangential stresses were highest and where seismic velocity (V_p) gradients were steepest. Relatively decreased velocities were seen in the two regions that were under tensile tangential stress. It is of particular interest to note the "broadness" of the high velocity regions, which presumably reflect an increase in deformation modulus due to the particular alignment of the maximum tangential stresses. Concurrence of AE events with high

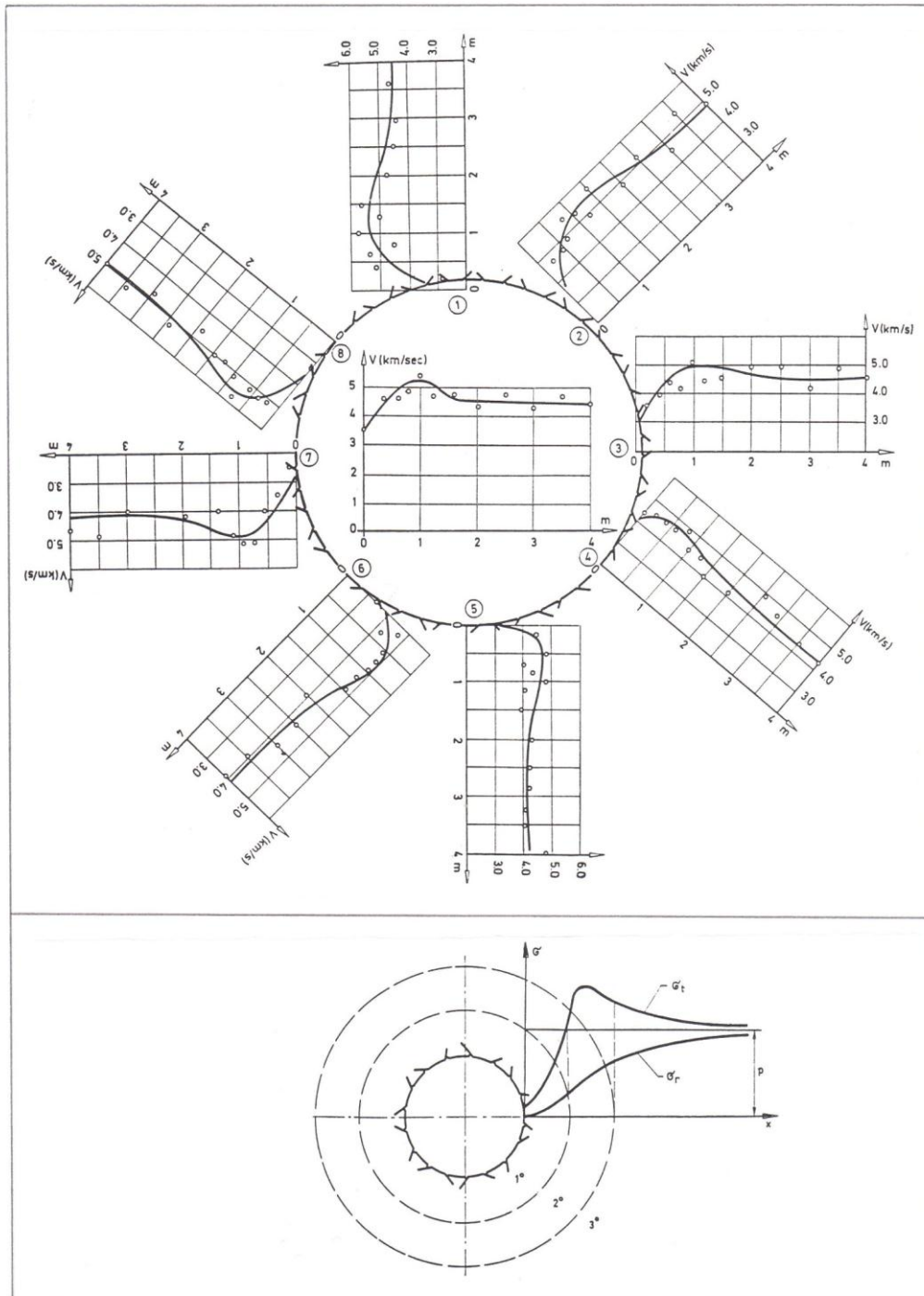


Figure 14. Excavation disturbed zone (EDZ) effects on cross-hole velocities in a pressure tunnel, and corresponding stresses. Kujundzic, (1970).

stress conditions ahead of the mining face in the South African Blyvoor gold mine, were again associated with high velocities (for example 5.8 - 5.9 km/sec) in the P-wave tomogram. Therefore using passive source (AE) tomography, the velocity image could potentially be used to map problem areas. The majority of small magnitude rock bursts in the mine were located in a region of high velocity gradient, between a low-velocity failed zone and high-velocity, highly-stressed zone. Logic would perhaps indicate that this was a region of high shear stresses.

Use of seismic refraction tomography for monitoring stress and stress change in mining seems to have started in the 1980's. Friedel et al (1996) describe its use for imaging apparent stress distributions and stress changes in yield pillars as a result of adjacent long wall coal mining. The velocity distribution in the yield pillar shown in Figure 16, ranging from 2 to 4 km/sec, suggests non-uniform stress. The reduced velocity along the side away from the working face was reportedly in general agreement with pressure cell measurements. The area of highest concentrated velocity (and therefore stress) was at the end of the pillar closest to the long wall face.

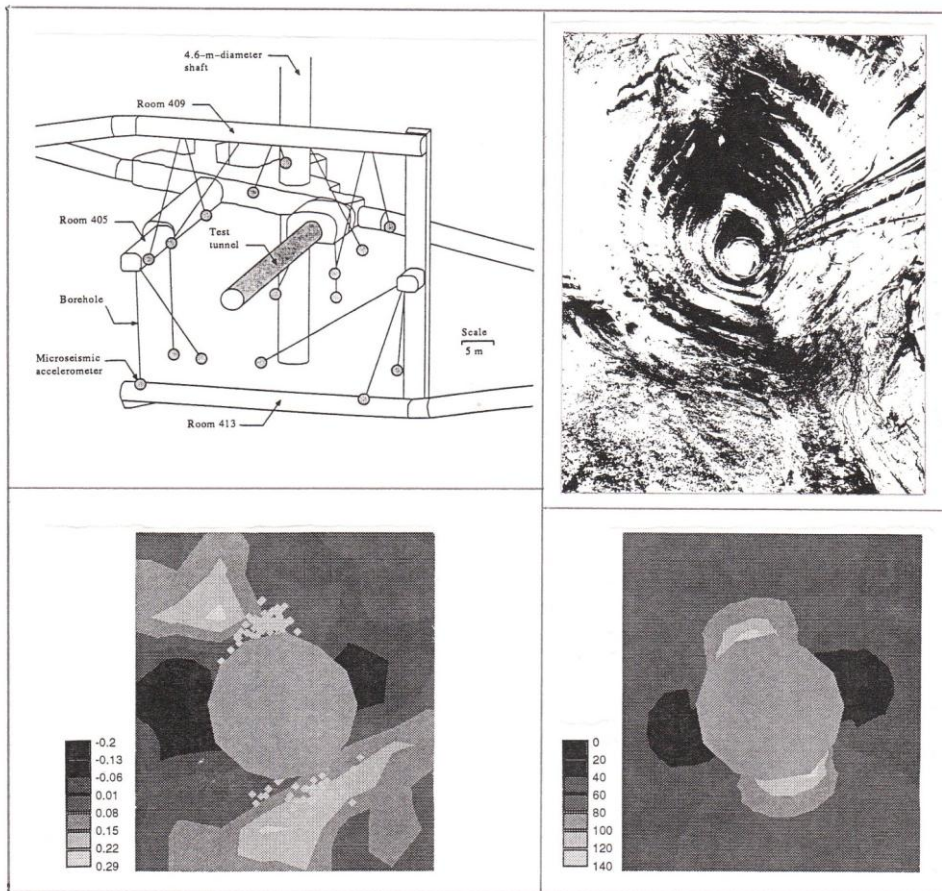


Figure 15. Utilization of passive wave AE tomography at URL line-drilled tunnel. Reduced velocities (left) and stresses (right) shown black, in contrast to light zones of high velocity and high stress. Note AE and dog-earing of the tunnel. Maxwell and Young, (1996).

In another study, Friedel et al (1995) describe three-dimensional tomographic imaging of anomalous stresses in a deep US gold mine. Their average velocity tomograms indicated a wide range of velocities (3.0 to 6.9 km/sec), with a sensible correlation of low velocities with drifts, stopes, ore shoots, and areas of rock burst damage. High velocity regions indicated regions where compressive stresses were obviously very high. The measurements were carried out between two levels of the mine at 2165 m and 2210 m depth.

In discussing the significance of seismic refraction tomography for monitoring stress change anomalies, Friedel et al (1995) warned that velocity gradients rather than high velocities, may be the best way to locate areas of imminent rock failure or rock burst. High differential stresses, which can be precursors of rock failure, are most probably associated with strong velocity gradients since in the σ_3 direction velocities may be low or even decrease in magnitude.

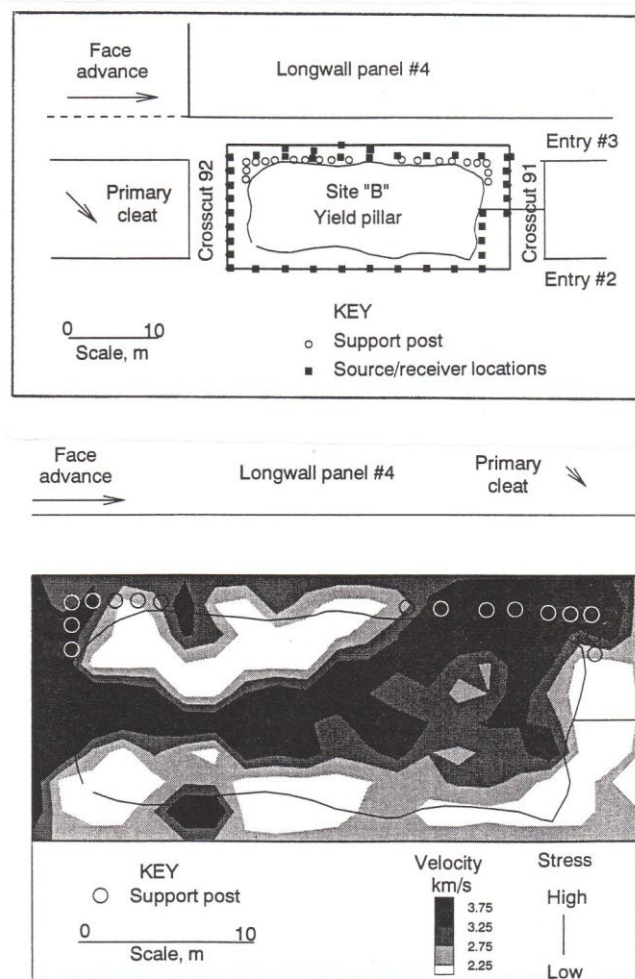


Figure 16. Cross-pillar seismic tomography for monitoring apparent stress changes from adjacent long wall mining advance. Friedel et al. (1996).

Strong velocity gradients under an indenter loading a cylinder of sandstone to 110 MPa are shown in an illustrative application of ultrasonic tomography by Scott et al (1994). Presumably the high velocity gradients caused by maxima of 3.55 km/sec compared to an unstressed 2.3 km/sec, are pre-cursors of failure. Their small-scale experimental set-up and key results are illustrated in Figure 17.

9. INTEGRATION OF VELOCITY, QUALITY, POROSITY, STRESS, STRENGTH AND DEFORMABILITY

It has been shown in previous sections how the P-wave velocity is sensitive to each of the factors listed above. To this we must also add moisture content (for the matrix) and ground water level (for the rock mass). The assumption will be made in the following development that seismic velocity measurements will frequently be made in saturated rock masses. The correlations developed will be based on this assumption, and errors will of course arise if drainage causes drying out of the matrix and/or joint water. The large velocity reductions sometimes seen in EDZ measurements, amounting to 2 or 3 km/sec may not correlate either to the less dramatic moduli reductions, or to the apparent rock quality reductions, specifically due to the moisture content changes that may have occurred following excavation. However, an order of magnitude reduction in deformation modulus may well occur in an EDZ due to radial de-stressing and other mechanical effects such as joint opening, and as shown earlier, this may be expected to strongly effect velocities, even if the joints remain fully saturated.

Since velocity - rock quality correlation is a complex task, no hesitation must be made in making some degrees of sophistication to the simple model $V_p = 3.5 + \log_{10} Q$ proposed earlier (Figure 2). Avoidance of mathematics suggests the use of a graphic method for correcting our hard, unweathered, low-porosity, near-surface rock masses (i.e. typical Sjøgren et al. 1979 data) to conditions towards the other end of the seismic and rock quality scale, e.g.: low strength, weathered, high porosity, highly stressed (or unstressed) rock masses.

The development shown in Figure 18, which is explained in detail by Barton 1996, has opposing corrections for porosity and depth (i.e. stress) since these cause opposing influences on velocity. In addition, an adjustment for uniaxial compression strengths different from a typical hard rock 100 MPa (or more) is made by the following simple adjustment to the Q-value:

$$Q_c = Q \cdot \frac{\sigma_c}{100} \quad (\sigma_c \text{ expressed in MPa}) \quad (1)$$

This correction is necessary because the Q-value for rock mass quality was originally developed for correlation with tunnel and cavern support needs. The Q-value uses the ratio strength/stress (σ_c/σ_1 in the SRF factor) only when stress levels are causing stress-related fracturing. It is probable that in a tunnel EDZ, the potentially large values of SRF (that reduce the Q-value directly) can also be used in principal to predict the measured reductions in velocity and deformation modulus. In such cases σ_c will be high for hard massive rocks subject to stress-slabbings, and σ_c will be low for soft rocks that are subject to squeezing.

The “opposed corrections” referred to in Figure 18 are designed to do the following:

1. $\sigma_c / 100$ corrects the Q-value to an approximately suitable value of Q_c to correlate more closely with deformation modulus (M) and with V_p , particularly for the case of softer rocks.

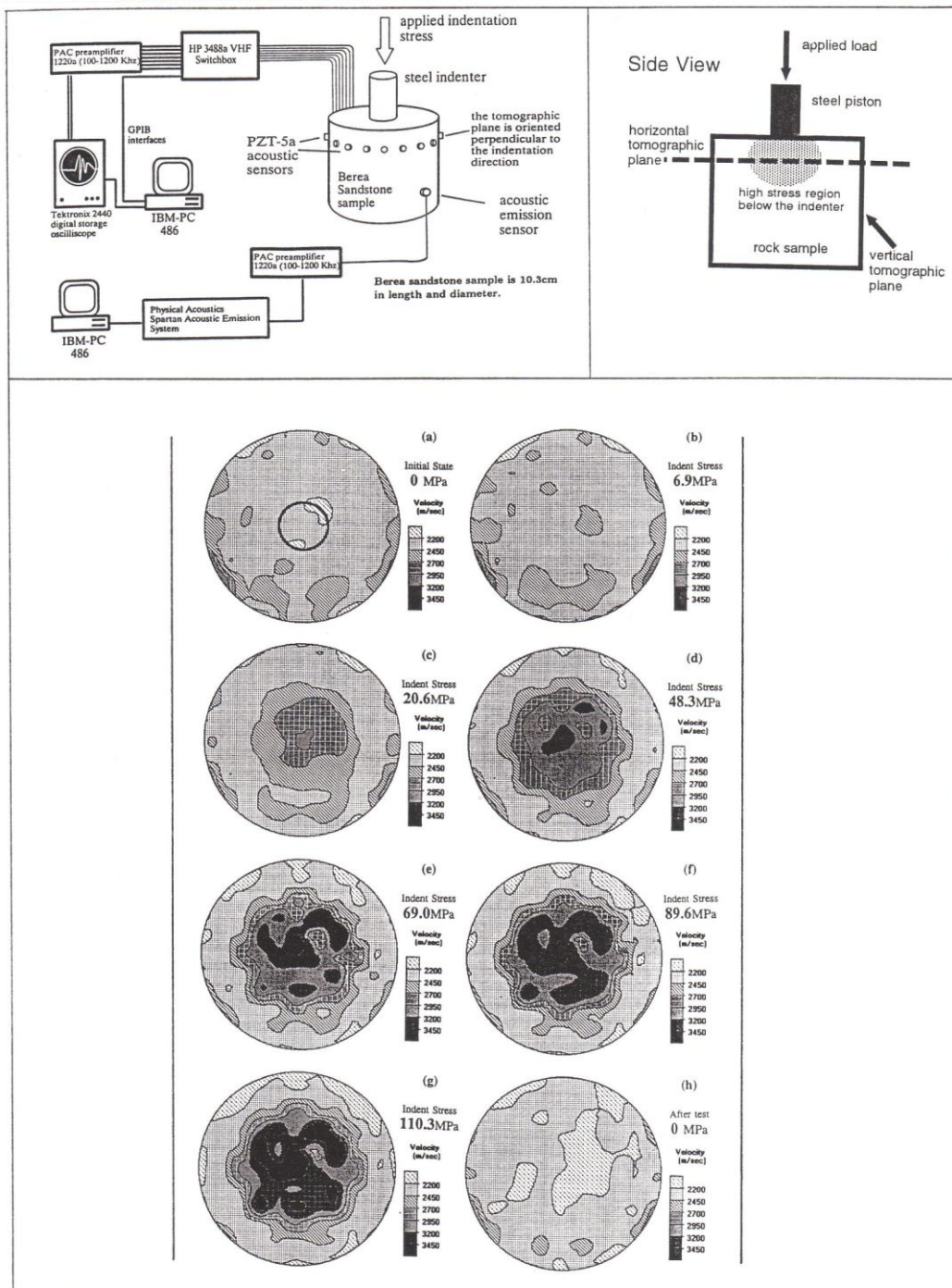


Figure 17. Ultrasonic tomography to monitor the loading of an indenter on Berea sandstone. Scott et al. (1994).

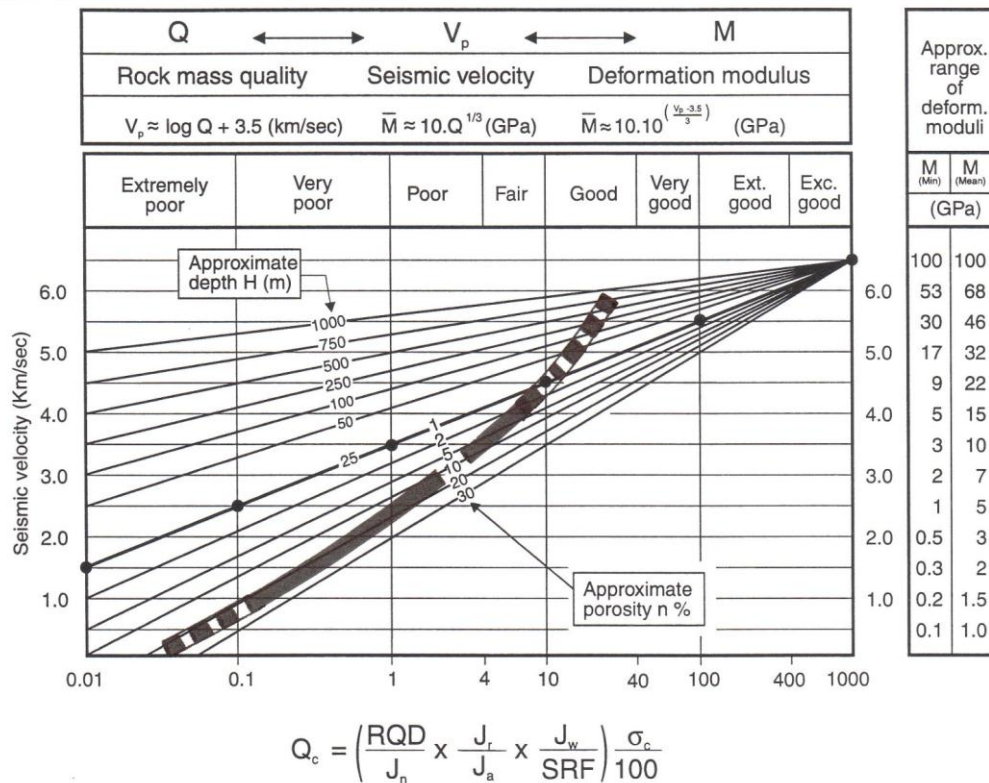


Figure 18. A method for linking rock quality, seismic P-wave velocity and deformation modulus with opposed corrections for strong or weak rocks (change σ_c), and opposed corrections for depth and porosity. Barton, (1995). A typical weathered profile is shown, with increased depth causing increased V_p , Q and M as a continuously varying process. (As shown later, in many cases Lugeon value $\approx 1/Q_c$).

2. A strongly non-linear depth correction gives greater sensitivity to “acoustic joint closure” for weaker and lower quality rock masses.
3. A weakly non-linear porosity correction also gives larger changes to velocity for the weakest rocks.

The chart, which should be considered as an approximate engineering guideline, was developed with the hard rock ($V_p = 3.5 + \log_{10} Q$) relationship (Figure 2) as a “core” (see black discs in Figure 18). Development for soft rocks occurred by a process of trial-and-error fitting of Q , V_p , σ_c , n and depth data from known sites in chalks (Saul Denekamp, pers.comm.), chalk marl, sandstones, mudstones, shales and tuff. Data from Israel, England, Japan and China were included. Depths ranged from about 25 meters to more than 1000 meters in the case of tuff/ignimbrite from UK Nirex’s Sellafield site, where cross-hole tomography and laboratory tests could be compared with NGI’s detailed Q-logging of 9 km of drill core.

The first two empirical relationships listed in the top of Figure 18 have been derived from extensive field test data for hard rocks (Barton, 1996). Testing with soft rocks has shown that the modified Q_c term gives satisfactory fit, which is improved when the porosity and depth corrections are also made. Thus we have:

$$V_p \approx \log_{10} Q_c + 3.5 \quad (\text{km/sec}) \quad (2)$$

$$M(\text{mean}) \approx 10 Q_c^{1/3} \quad (\text{GPa}) \quad (3)$$

Although there is little data for deformation modulus measurement at “undisturbed” depths of hundreds of meters, it will be noted that these predicted static moduli become closer to the seismically derived dynamic E modulus (from V_p , V_s and density). If truly undisturbed static modulus testing could be achieved, the normal discrepancy between static deformation modulus and dynamic E modulus might be lessened, despite the fundamentally different levels of strain involved in each case.

An illustration of application of the Q - V_p - M method to very soft rocks can be given here, based on Q-logging of tunnels in chalk marl (Terlingham, Beaumont and UK-sector Channel Tunnels, and selected marine drill core; PB1 to PB8). Details of the logging are given by Barton and Warren, 1996.

A weighted mean value of $Q = 8$ was obtained from the so-called “predecessor-study” of available tunnels and core. This was found to compare closely with the over-all mean Q-value of the contractor-owner (TML-ET) TBM face logs from the troublesome (water and over-break) km 20-24 sub-sea chainage, where an overall mean value of $Q = 9$ was obtained from the three machine-bored tunnels. The mean σ_c value for the chalk marl was 6 MPa. Thus we have:

$$\bar{Q} = 8, \quad \bar{\sigma}_c = 6 \text{ MPa}, \quad \bar{Q}_c = 8 \times \frac{6}{100} = 0.48$$

This Q_c value intersects the central diagonal line (equation 2) in Figure 18 at $V_p = 3.2$ km/sec. Correction for average porosity ($n = 27.7\%$) results in a reduction of 1.6 km/sec giving $3.2 - 1.6 = 1.6$ km/sec. Tunnel depths of, for example 40 m, bring this value up to about 2.0 or 2.1 km/sec. Offshore geophysics carried out during several campaigns indicated P-wave velocities generally in the range 2.0 to 2.6 km/sec for the UK chalk marl. A Q-value of about 20 is needed to explain the upper velocity of 2.6 km/sec using the above method, which is in line with the otherwise generally good qualities registered outside the 4 km zone with much over-break.

Lugeon testing had indicated a typical range of 1 to 20 Lugeons in the jointed chalk marl which has negligible matrix permeability due to the clay content. If we invert these Lugeon values and tentatively express them as $Q_c \approx 1$ to 0.05, we see the outlines of a method of correlating V_p - Q_c - $1/\text{Lugeon}$ - M. The predicted moduli of $M \approx 0.5$ GPa (minimum) and 3 GPa (mean) compare with (disturbed) but unjointed laboratory scale moduli of 0.64 GPa (mean) and 0.15 to 4.2 GPa (range). Deformation in the tunnels were interpreted as indicating an in situ modulus of about 1 to 2.5 GPa for a range of rock qualities.

10. POTENTIAL V_p - Q - LUGEON CORRELATION

Dam sites throughout the world are investigated by means of borehole water injection tests, typically using double packers, and injection-pressures related to depth below the surface, but usually limited to about 0.25 or 0.5 or 1.0 kg/cm² per meter depth. The number of Lugeons is expressed by the well known relation $L = \text{litres/min/m/1 MPa excess pressure}$. Most of the flow losses (and joint deformation) occur close to the borehole in such a test, which differs greatly from the careful, low pressure pumping extraction tests favoured in permeability testing (Quadros et al. 1995).

By good fortune or correct physics, the modulus of deformation (M) shown in Figure 18 and equation 3 is proportional to $Q^{1/3}$ or to $Q_c^{1/3}$ in the case of rocks weaker or stronger than our nominal $\sigma_c = 100 \text{ MPa}$. Similarly, it is well known that flow rate is more or less proportional to e^3 in jointed rock masses (where $e = \text{equivalent hydraulic aperture of the joints}$). The smaller value of (e) approaches the physical aperture (E) when $e \approx 1.0 \text{ mm}$, and this inequality ($E/e \geq 1$) is related to joint roughness JRC (Barton et al. 1985).

Around the injection borehole we may assume that the natural joint apertures are deformed significantly, especially when maximum injection pressures of 0.025 up to 0.1 MPa per meter depth are used. The latter European injection pressure limit at dam sites is about 0.4 to 0.5 times the assumed vertical total stress, and when $k_o (= \sigma_h/\sigma_v)$ is less than these figures, or even just close to them, some hydraulic jacking of some of the joints is an obvious consequence in the initial radii around the boreholes.

The following basic assumptions will be made concerning this all important joint deformation region around the injection holes:

1. The Lugeon value (L) which is recorded as volumetric flow rate (litres/min) will tend to be proportional to the cube of the new apertures that have been created i.e. $\alpha(\Sigma E^3)$. There is some evidence that the most permeable and well connected joints open most at the expense of others in the same set. The resulting Lugeon value will often be dominated by the E(max) value and we can roughly approximate here that $L \propto E^3_{\text{max}}$.
2. The gapped joint will have an aperture E(max) that is approximately inversely proportional to deformation modulus M, unless $k_o (= \sigma_h/\sigma_v)$ is very low and real hydraulic jacking has occurred.

Therefore we have the following possibilities of inter-relationships between maximum apertures, Lugeon values, deformation moduli and Q-values, which in turn are linked to seismic velocities:

	L	α	E^3_{max}
	E_{max}	α	M^{-1}
	M	α	$Q_c^{1/3}$
Therefore	L	α	Q_c^{-1}

(Note “ α ” implies “approximately proportional to”, in the above proportionalities).

These simple proportionalities suggest that the number of Lugeons may be proportional to $1/Q_c$, unless other mechanisms than local joint deformation are responsible for the flows, for example outwashed chlorite fillings, severely channelized flow due to basalt flow-top weathering, and so on.

Velocity measurements sometimes correlate closely with injectability and are often used for monitoring the success or otherwise of grouting. At the 270 m high Inguri arch dam in Georgia, Savich et al. (1983) used the seismic velocity criteria shown in Figure 19 for judging the success of grouting. One can first interpret that very high pressures must have been used here, since it is implied that velocities as high as 4.5 km/sec can be improved by grouting. However the depth effect on V_p (Figure 18) is probably playing a role. A V_p value of 4.5 km/sec implies $Q_c = 10$ in near-surface hard, unweathered rocks. However at the 270 m high dam, deep injection grouting and deep V_p monitoring (say at 100 to 200 m depth) might have had a depth (stress) related enhancement that was equivalent to a much lower rock quality of $Q_c = 1$ or even less, which is likely to be injectable. Savich et al. (1983) results are therefore readily understandable when the V_p - Q - depth effect is taken into account.

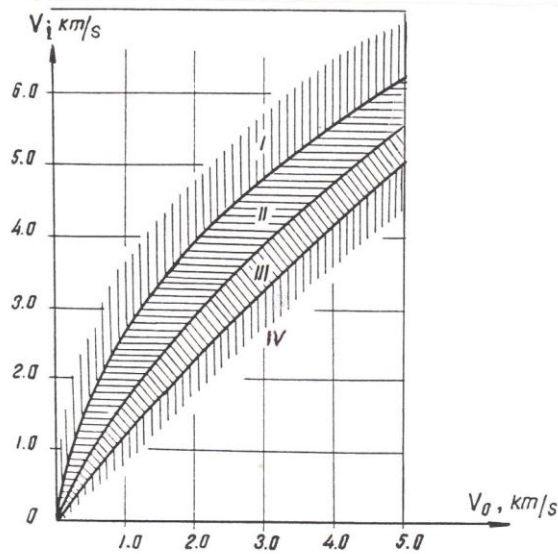


Figure 19. Grouting efficiency monitored by V_p at the 270 m high Inguri arch dam in Georgia. (I = excellent, II = good, III = satisfactory, IV = unsatisfactory). Savich et al. (1983).

Extensive sets of in situ measurements concerning foundation moduli, permeability and seismic velocity were assembled by the French National Group (1964) from numerous dam site investigations. For the special case of two sites in jointed granite (from France's Massif-Central), a strong correlation was evident between V_p and the Lugeon test results. Figure 20 shows an approximately linear distribution of data on a semi-log plot of V_p versus the Lugeon value. If we make the assumption that shallow refraction seismic, or relatively shallow cross-hole measurements of velocity were used, then we can tentatively investigate the relation $V_p \approx 3.5 + \log_{10} Q_c$ (the diagonal line in Figure 20) as a means of relating Q -value and Lugeon value. In very approximate terms we can see from the data that not only proportionality, (i.e. $L \propto 1/Q$) but equality $L \approx 1/Q$ is evident in the approximate range 100 to 1.0 Lugeon. The scatter of velocities and Q -values is seen to be about one order of magnitude, in other words neither velocity measurement, nor Q -logging must be substituted for the testing. However $L \approx 1/Q$ (Lugeon) might be utilized in extrapolation exercises, or to identify non-conforming behaviour.

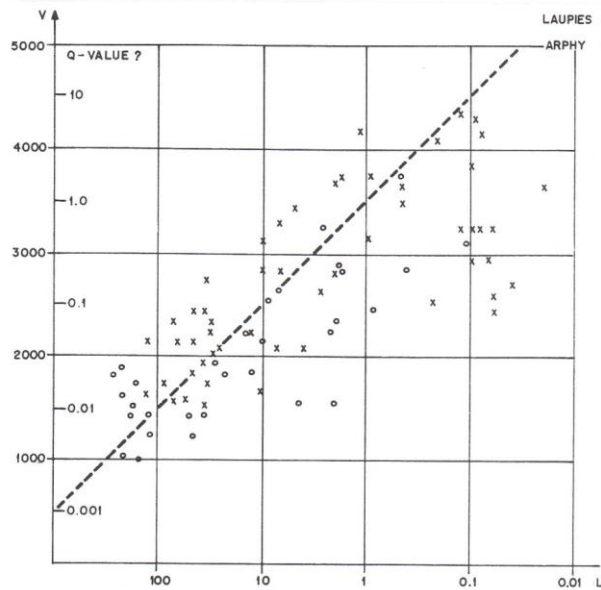


Figure 20. Correlation between V_p and Lugeon number at two dam sites on jointed granites. French National Group. (1964). (The diagonal line and tentative Q-values has been added here).

We may therefore tentatively write:

$$L \approx \frac{1}{Q} \text{ (Lugeons)} \quad (4)$$

as a useful approximate for fitting to data in some rock masses, and for explaining deviation (i.e. extreme channelling in other cases).

Since discovering the proportionality/equality rule-of-thumb described above, a lot of Lugeon testing has been scrutinized, and a few examples will be given.

Swolf et al. (1981) reported on a well controlled in situ 2 m^3 block test in sandstone, with simultaneous stress application (to 2 MPa) velocity monitoring, permeability measurement, and deformability testing. The values of L , V_p , M and the estimated Q-value from the description of the site are all approximately consistent with the $V_p - M - Q - L$ model described above.

Two campaigns of core drilling for a shallow tunnel through meta-sediments in the UK, first with vertical holes then with 45° inclined holes (to intersect more of the steep structure) gave mean Lugeon results of 12 and 28. If we assume $Q \approx 1/L$, then Q values of about 0.08 and 0.04 are predicted. Completely independent Q-logging of core from the relevant boreholes (8 from phase 1 vertical holes, and 13 from phase 2 inclined holes) gave weighted mean Q-values from many hundreds of observations as follows:

$$\begin{aligned} Q \text{ (BH 1 to 8)} &= 0.11 \\ Q \text{ (BH 13 to 21)} &= 0.08 \end{aligned}$$

The tunnel itself subsequently showed an overall weighted mean Q-value of 0.05. Downhole V_p logging in BH 1 to 8 gave a mean V_p of 2.58 km/s for the same depth ranges that were Q-logged. This converts to a predicted Q-value (using equation 2) of 0.12, almost exactly as logged.

The above logging data shows remarkable similarities to the $L \approx 1/Q$ model, and also shows the potential anisotropy of the Q-value due to different joint sampling frequency with hole orientation. Higher Q-values, lower Lugeon values, and higher seismic velocities will tend to be measured when sub-parallel to major structure. The opposite occurs when crossing major structure. Of course there are likely to be exceptions to this basic concept caused primarily by stress-anisotropy.

At four hard rock sites investigated by Sjøgren et al. (1979) in Norway shown in Figure 21, the curved $L \approx 1/Q$ envelope obtained from $V_p \approx 3.5 + \log_{10} Q$ is found to be a lower bound to the data. These two approximate equations can be combined in the following form to fit such data:

$$L \approx 10^{(3.5 - V_p)} \quad (\text{Lugeons}) \quad (5)$$

However, the approximate influence of depth on V_p (Figure 18) for any given Q-value should always be remembered when testing this simple relationship.

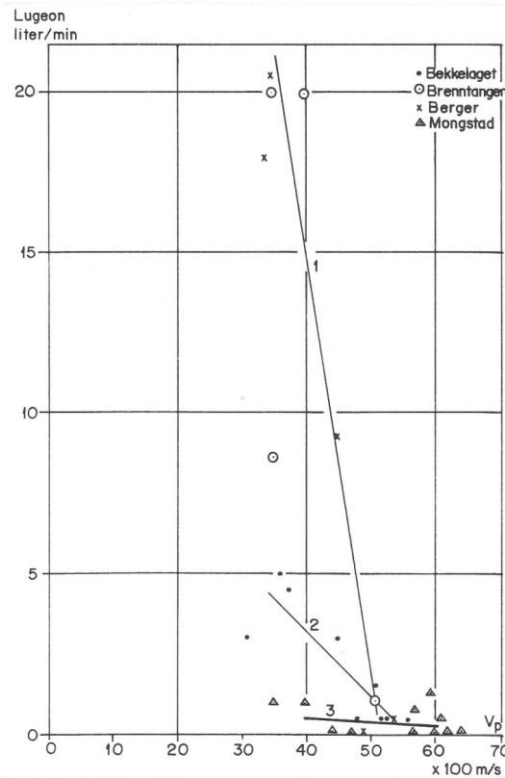


Figure 21. An attempt at correlating Lugeon values at hard rock sites with V_p values. Sjøgren et al. (1979).

At the Chinnor Tunnel in chalk marl (Figure 1) Hudson et al. (1980) referred to very low velocities (0.6 to 1.0 km/sec) for badly fractured/jointed areas of the chalk marl and quoted permeabilities from Lugeon type tests of 10^{-4} to 10^{-6} m/sec in these areas. If we assume for simplicity that 1 Lugeon $\approx 10^{-7}$ m/sec, then the very high Lugeon values obtained of 1000 to 10 imply Q_c values of 0.001 to 0.1 according to equation 4. These low Q_c values can be converted to

“tunnelling” Q values of 0.02 to 2 if we assume a mean σ_e value of 5 MPa for the chalk marl. This range is in line with expectations for the heavily jointed rock mass at Chinnor.

11. ENGINEERING IMPLICATIONS OF V_p - Q - M - L COUPLING

Some remarkably simple but obviously only approximate relationships have been developed in this paper, some of which may require further refinement and the benefit of reflection. On the face of it, critics may think it unreasonable to assume that “permeability” has anything to do with either rock quality Q or with seismic velocity V_p . This critique is justified concerning the intrinsic almost undisturbed permeability that can be measured by careful pumping (extraction) testing at small under-pressures. In this paper however, the assumption is made that the Lugeon test is more a deformability test than a permeability test and therefore is likely to be related in some way to each of the parameters under discussion (V_p , Q and M).

Another question that may be raised is the effect of grouting. Most engineers know from experience that correctly carried out grouting reduces leakage, and that it increases deformation modulus and probably shear strength, since tunnels that are pre-injected show each of these characteristics, and the same is probably true in dam foundations. In the tunnel situation, the need for support is obviously reduced, and tunnel deformation is reduced. Since tunnel deformation is closely linked to SPAN/Q (Barton et al. 1994) and support needs are linked directly to Q, the inescapable conclusion (which would also be arrived at by velocity monitoring and deformability testing) is that the effective Q-value has been increased by the pre-injection.

The Q-value is determined from RQD, the number of joint sets, (J_n), the roughness (J_r) and degree of alteration (J_a) of the least favourable set, and from the water inflow (J_w) and stress/strength condition (SRF). From Figure 18, a velocity increase of 1 km/sec from say 3.5 to 4.5 km/sec at a dam site, or in a wet, jointed zone ahead of a large tunnel, will imply that the Q-value has increased from 1 to 10 as a result of the grouting. Following equation 5, a drop in Lugeon value from 1.0 to 0.1 is also implied, and using equation 3, the modulus of deformation may be predicted to have increased from 10 GPa to at least 20 GPa. Are these changes possible to explain via changes in the six component Q-parameters? The answer is definitely yes, but the exact answer will always be unknown. We could speculate that approximately the following may occur in principle:

1. RQD of 30% increases to 60% due to grouting of the most prominent set of joints that were most permeable.
2. J_n of 15 (four sets) is effectively reduced to 9 (three sets) for the same reason as above.
3. J_r of 1.5 (rough, planar) changes to 2 (another set) or to 4 (discontinuous).
4. J_a of 2 (weathered) changes to 1 (another set) or to 0.75 (cemented).
5. J_w of 0.5 (high pressure inflow) changes to 0.66 (small inflow).
6. SRF of 1 (unchanged). (In the case of a minor fault even SRF might change).

We therefore have the following potential “before” and “after” scenarios:

$$Q_1 = \frac{30}{15} \times \frac{1.5}{2} \times \frac{0.5}{1} = 0.8$$

$$Q_2 = \frac{60}{9} \times \frac{2 \rightarrow 4}{1 \rightarrow 0.75} \times \frac{0.66}{1} = 9 \rightarrow 23$$

The effective Q value has increased, which is broadly consistent with the increased V_p and M values, and with the reduced Lugeon value and rock support needs.

Examples of correlations between seismic refraction surveys and drilling and tunnelling results are also given by Sjøfgrén (1984). A good example is that reproduced in Figure 22 a, b and c. The need to site a water supply tunnel beneath the Skien river in Norway resulted in the four seismic refraction profiles shown in the top figure. Three low velocity zones were indicated beneath the river, the largest of which ($V_p = 2.5$ km/sec) was proved by an inclined borehole to be a partly

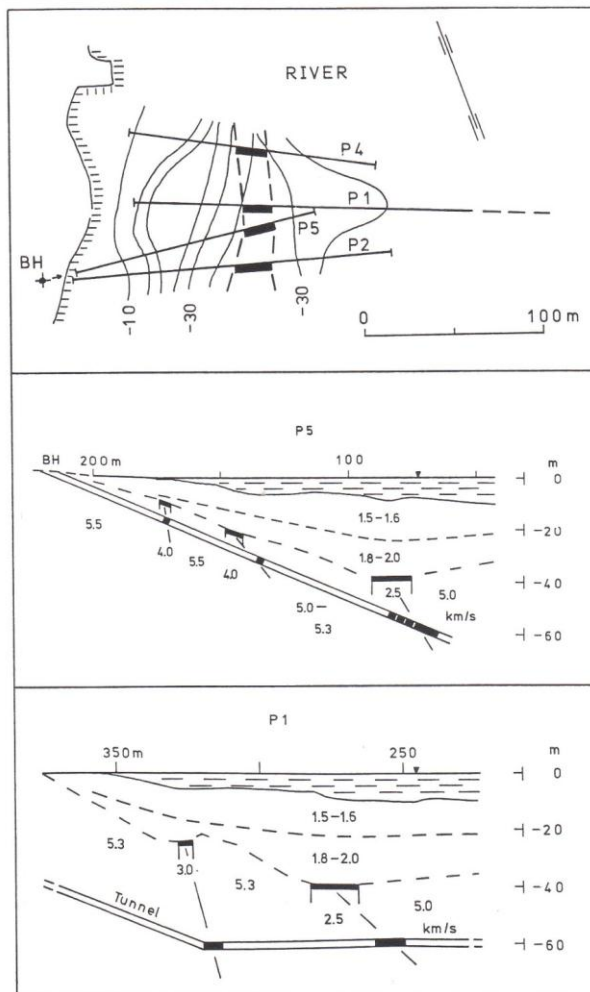


Figure 22. Drilling for confirmation of low seismic velocity, and subsequent tunnelling through the same zones in Norway. Sjøfgrén, (1984).

consolidated breccia and loose alum shale (core loss averaged 75% in this zone). The Lugeon value in this zone was 14, which might correspond to a Q_c value of about $1/14$ (≈ 0.07). This is close to the value of Q that could be predicted from Figure 18 using a nominal porosity for the zone of 5%, and the 50m depth shown in Figure 22 c. At this depth (and with $n = 5\%$) $Q = 0.07$ corresponds to $V_p = 2.5$ km/sec, as measured, by chance or good physics. The tunnel was driven through the same zone, in the direction of profile 1 (Figure 22 c). Grouting was necessary for the $V_p = 3.0$ km/sec zone. Probe drilling and heavy reinforcement was used through the 12 m wide fractured alum shale zone, which had $V_p = 2.5$ km/sec.

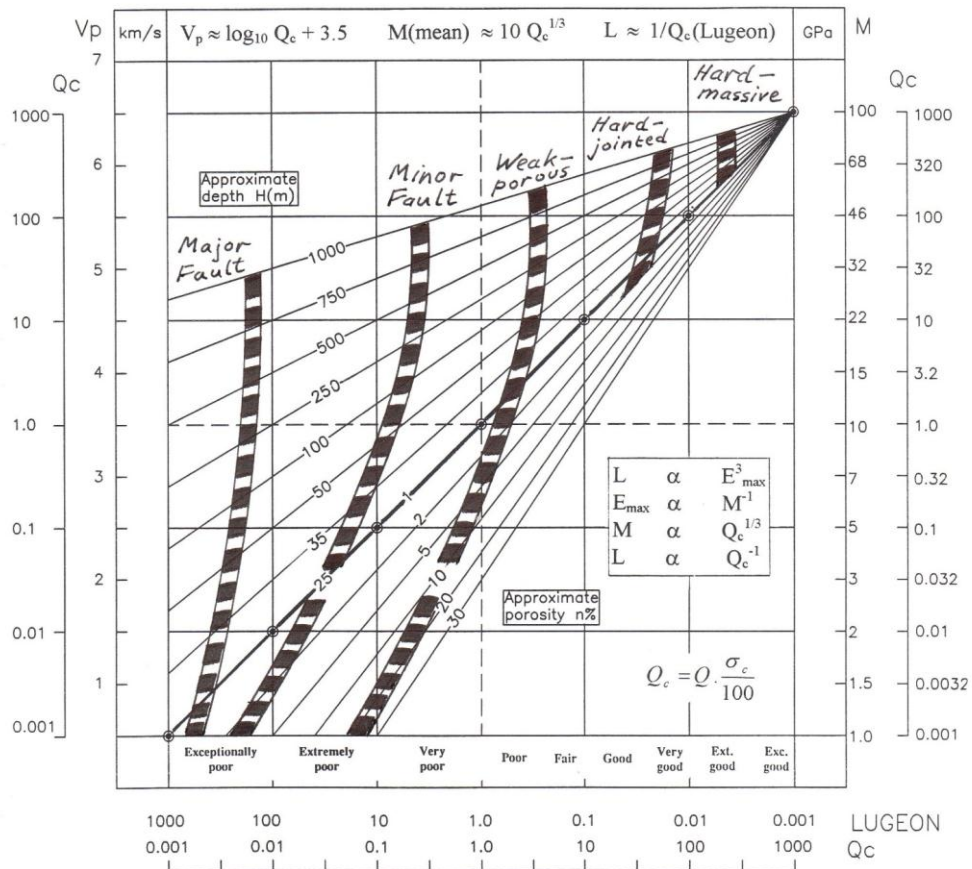


Figure 23. Summary of the integrated rock mass quality assessment method, using (or producing) V_p , Q_c , M and L estimates, based on corrections for depth, porosity and uniaxial strength.

12. DISCUSSION

The integrated model linking Q - M - V_p - L developed in this paper has further links to problems in rock engineering, due to one further set of observations from many hundreds of tunnel and cavern case records. The deformation recorded when driving a tunnel or cavern is strongly influenced by the rock mass quality and associated support requirements. Careful numerical modelling has shown that support in the form of rock bolts and shotcrete, even when placed close to or at the tunnel face is incapable of preventing deformation but is chiefly of benefit in preventing failure. In other words the rock mass responds in a quality-based manner to the almost irresistible forces of stress redistribution. Our support measures help to maintain integrity during this process but they cannot resist the process. The recorded deformation is therefore very much a function of the rock quality, of its shear strength and deformability, all of which can be broadly described by the Q-value.

In fact it has been found from these hundreds of case records that the central trend of behaviour follows the following relation (Barton 1998).

$$\Delta(mm) \approx \frac{SPAN(m)}{Q} \quad (6)$$

Exceptions are caused by anisotropic stresses, unsafe designs, adverse stress/strength ratios and so on.

Since we have the following approximations already:

$$L = 1/Q \quad M \approx 10 \cdot Q^{1/3} \quad \text{and} \quad V_p \approx \log_{10} Q + 3.5$$

the following intriguing potential relationships can be derived:

$$\Delta(mm) \approx SPAN \cdot L \quad (7)$$

$$\Delta(m) \approx SPAN/M^3 \quad (8)$$

$$\Delta(mm) \approx SPAN \cdot 10^{3.5 - V_p} \quad (9)$$

where SPAN is in meters, L is Lugeons, M is in GPa, V_p is km/sec.

These equations (approximations) are apparently indicating that the Lugeon test may indeed be more a deformation test than a permeability test, and that deformation is inversely proportional to modulus cubed. (It is tempting to speculate that a three-dimensional modulus is involved, and that we could use M₁, M₂ and M₃ to obtain a better result from anisotropic stiffnesses).

Although the case records involved do not specifically link tunnel deformation Δ with L or M, the linkage of Δ with Q, and Q with L and with M may justify the simplicity of the above relations. Since the approximations can be easily remembered in the field, it may be worth while testing their validity, since deviation from simple trends can sometimes be instructive, and help to develop improvements where needed.

13. CONCLUSIONS

1. The engineering applications of seismic velocity measurements have been reviewed. The rock mass characteristics that can be related to P-wave velocities, with most sensitivity at shallow depth, are joint frequencies, RQD, Q-value, Lugeon value, deformation modulus.
2. Complicating factors that must be carefully allowed for include the influence of the rock matrix parameters (σ_c , n% or density), the anisotropy (of microcracks, schistosity, jointing or stress), the degree of saturation and the depth. Acoustic "closure" of joints occurs at shallower depth for weaker rocks, and the sensitivity of V_p to rock mass properties generally reduces at greater depth, where P-wave amplitude may then be better than P-wave velocity in sensing joints.
3. A simple model has been derived linking V_p and the rock mass quality Q-value. This is modified by depth, porosity and the uniaxial strength of the rock.
4. A simple but more comprehensive model linking V_p , Q, modulus of deformation M and Lugeon value L has also been derived, and tested against some cases reported in the literature. The assumption is made that the Lugeon test is more a deformability test than a permeability test. Coupling is therefore established between V_p , Q, M, L and depth. The effect on each of these parameters of pre-grouting a low-velocity zone ahead of a tunnel face is assessed, including an analysis of potential changes to the individual Q-system parameters, caused by the grouting process.

14. ACKNOWLEDGEMENTS

Helpful discussion and some soft rock velocity and modulus data were received from Barry New (UK) and Saul Denekamp (Israel). Partial support for this study was received from the Norwegian Research Council, NFR under the project "Tunnel Seismic". Colleagues Harald Westerdahl (NGI) and Eda de Quadros (IPT) provided necessary and welcome support.

REFERENCES

- Aydan, Ö., Akagi, T., Ito, T., Kawamoto, (1992). Prediction of tunnels in squeezing ground. *Journal of Geotechnical Engineering, JSCE*, No. 448-19, pp. 73-82.
- Barton, N., S. Bandis, K. Bakhtar, (1985). Strength, deformation and conductivity coupling of rock joints, *Int. J. Rock Mech. Min. Sci. and Geomech. Abstr.* Vol. 22, No.3, pp-121-140.
- Barton, N., 1991, *Geotechnical Design*, World Tunnelling, November 1991, pp. 410-416.
- Barton, N., E. Grimstad, G. Aas, O.A. Opsahl, A. Bakken, L. Pedersen and E.D. Johansen, 1992, *Norwegian Method of Tunnelling*, WT Focus on Norway, World Tunnelling, June/August 1992.
- Barton, N., T.L. By, P. Chryssanthakis, L. Tunbridge, J. Kristiansen, F. Løset, R.K. Bhasin, H. Westerdahl, G. Vik, 1994, Predicted and Measured Performance of the 62m span Norwegian Olympic Ice Hockey Cavern at Gjøvik, *Int. J. Rock Mech, Min. Sci. & Geomech. Abstr.*, Vol. 31, No. 6, pp. 617-641. Pergamon.
- Barton, N. 1995. The Influence of joint properties in modelling jointed rock masses. Keynote lecture. *Proc. 8th ISRM congress, Tokyo*. 3: 1023-1032. Rotterdam: Balkema.
- Barton, N. and C. Warren, 1996, Rock Mass Classification of Chalk Marl in the UK Channel Tunnels, *Channel Tunnel Engineering Geology Symposium*, Brighton, September 1995.
- Barton, N., 1996, Estimating Rock Mass Deformation Modulus for Excavation Disturbed Zone Studies, *International Conference on Deep Geological Disposal of Radioactive Waste*, Winnipeg, 1996.

- Barton, N. (1998). NMT support concepts for tunnels in weak rocks . Proc. of ITA World Congress, São Paulo, Brazil.
- Emsley, S.J., Olsson, O., Stanfors, R., Stenberg, L., Cosma, C. & Tunbridge, L. 1996. Integrated characterisation of a rock volume at the Äspö HRL utilised for an EDZ experiment. *Eurock '96*. Barla (ed.) 2: 1329-1336. Rotterdam: Balkema.
- Fourmaintraux, D. 1995. Quantification des discontinuités des roches et des massifs rocheux. *Rock Mechanics*, Vol. 7, pp. 83-100.
- French National Group, 1964. "La deformabilite des massifs rocheux. Analyse et comparaison des resultats". 8th Int. Cong. on Large Dams, Edinburgh Vol.1, R.15, Q.28.
- Friedel, M.J., Scott, D.F., Jackson, M.J., Williams, T.J. and Killen, S.M. 1995. 3D tomographic imaging of mechanical conditions in a deep US gold mine. *Mechanics of Jointed and Faulted Rock*. International Conference on the Mechanics of Jointed and Faulted Rock, 2. Vienna 1995. Pp. 689-695. Rotterdam, Balkema.
- Friedel, M.J., Jackson, M.J., Williams, E.M., Olson, M.S. & Westman, E. 1996. Tomographic imaging of coal pillar conditions: Observations and implications. *Int. J. Rock Mech. Min. Sci. & Geomech. Abstr.* 33: 3: 279-290. UK: Pergamon.
- Hasselström, B., Rahm, L. and Scherman, K.A. 1964. Methods for the determination of the physical and mechanical properties of rock. *International Congress on Large Dams*, 8. Edinburgh 1964. Vol. 1, Q. 28, pp. 611-625. Paris, ICOLD.
- Helfrich, H.K., B.Hasselström and B. Sjøgren. (1970). Complex geoscience investigation programmes for siting and control of tunnel projects . *The Technology and Potential of Tunnelling*, Vol. 1 (ed. N.G.W. Cook), Cygnet Print Ltd. Johannesburg.
- Hesler, G.J., Cook, N.G.W. & Myer, L. 1996. Estimation of intrinsic and effective elastic properties of cracked media from seismic testing. *2nd NARMS '96. Montréal, Québec*. Aubertin, Hassani & Mitri (eds). 1: 467-473. Rotterdam: Balkema.
- Hudson, J.A., Jones, E.J.W. and New, B.M. 1980. P-wave velocity measurements in a machine-bored, chalk tunnel. *Quarterly J of Engineering Geology*, Vol. 13, pp. 33-43.
- King, M.S., Myer, L.R. and Rezowalli, J.J. 1984. Cross-hole acoustic measurements in basalt. *Rock Mechanics in Productivity and Protection*. Symposium on Rock Mechanics, 25. Evanston, Ill. 1984. Pp. 1053-1061. New York, Society of Mining Engineers of AIME.
- New, B.M. and West, G. (1980). "The transmission of compressional waves in jointed rock". *Eng. Geol.* 15, pp. 151-161.
- Niini, H. and Manunen, T. 1970. Seismic sounding as indicator of engineering-geologic properties of bedrock in Finland. *International Association of Engineering Geology*. International Congress, 1. Paris 1970. Vol. II, pp. 753-761.
- Nur, A. 1971. Effects of stress on velocity anisotropy in rocks with cracks. *J of Geophysical Research*, Vol. 76, No. 8, pp. 2022-2034.
- Oberti, G., Carabelli, E., Goffi, L. and Rossi, P.P. 1979. Study of an orthotropic rock mass: experimental techniques, comparative analysis of results. *International Society for Rock Mechanics*. International Congress, 4. Montreux 1979. Vol. 2, pp. 485-491. Rotterdam, Balkema.
- Palmstrøm [Palmstrong], A. 1996. Application of seismic refraction survey in assessment of jointing. *Conference on Recent Advances in Tunnelling Technology*. New Delhi 1996. Vol. I, pp. 15-22. New Delhi, Ministry of Water Resources.
- Quadros, E. F. (1995). Water Percolation in Rock Foundations in Brazil. Special Lecture in the 8th ISRM Congress, Tokyo, Japan, 1995. Workshop on Rock Foundation.
- Sato, J., Itoh, J., Aydan, Ö. and Akagi, T. (1995). Prediction of time-dependent behaviour of a tunnel in squeezing rocks . *FMGM'95, 4th Int. Symp. Bergamo, Italy*.
- Saito, T. 1981. Variation of physical properties of igneous rock in weathering. *Proc. Int. symp. on weak rock, Tokyo*. 191-196.

- Scott Jr., T.E., Ma, Q., Roegiers, C. & Reches, Z. 1994. Dynamic stress mapping utilizing ultrasonic tomography. *1st NARMS '94. Austin Texas*. Nelson & Laubach (eds). 427-434. Rotterdam: Balkema.
- Sjøgren, B., Øfsthus, A. and Sandberg, J. 1979. Seismic classification of rock mass qualities. *Geophysical Prospecting*, Vol. 27, pp. 409-442.
- Sjøgren, B. 1984. *Shallow refraction seismics*. London, Chapman & Hall. 268p.
- Stapledon, D.H. and Rissler, P. 1983. Site exploration and evaluation. General report. International Society for Rock Mechanics. International Congress, 5. Melbourne 1983. Vol. 3, pp. G5-G25. Rotterdam, Balkema.
- Swolfs, H.S., C.E. Brechtel, W.F. Brace, and H.R. Pratt, (1981). Field mechanical properties of a jointed sandstone. *Mechanical Behaviour of Crustal Rocks*, Geophysical Monograph 24, Am. Geophys. Union. Pp.161-172.
- Tanimoto, C. and Ikeda, K. 1983. Acoustic and mechanical properties of jointed rock. International Society for Rock Mechanics. International Congress, 5. Melbourne 1983. Vol. 1, pp. A15-A18. Rotterdam, Balkema.
- Tanimoto, C. & Kishida, K. 1994. Seismic geotomography: Amplitude versus velocity in consideration of joint aperture and spacing. *1st NARMS '94. Austin Texas*. Nelson & Laubach (eds). 147-155. Rotterdam: Balkema.

ROCK MASS CHARACTERIZATION FROM SEISMIC MEASUREMENTS

ABSTRACT

A wide ranging review of seismic measurements in rock engineering projects has been undertaken using literature from the last thirty years or so. This summary paper focuses on rock mass conditions that can be deduced from surface refraction seismic, cross-hole tomography and excavation disturbed zone (EDZ) studies around tunnels. A correlation is developed between P-wave velocity and the anisotropic rock mass quality Q , with allowance for the opposing effects of depth and porosity and high or low compression strength. The deformation modulus M is included in the correlation. The V_p - Q - M correlation model is extended on the basis of reviewed data to include the Lugeon value (L) which is more a joint deformation test than a permeability test. The integrated V_p - Q - M - L correlation model allows rock masses to be given an approximate type curve, from near surface to 1 km depth. Wide separation of hard massive rock, jointed rock, weak porous rock and faulted rock is seen in these type curves, which show strongest changes of V_p , Q , M and L in the weathered zone.

Key words: seismic velocity - rock quality - Q -value - tunnels - anisotropy - deformation-weathering-excavation disturbed zone (EDZ) - grouting